Binding Dynamics at the Quinone Reduction (Q_i) Site Influence the Equilibrium Interactions of the Iron Sulfur Protein and Hydroquinone Oxidation (Q_o) Site of the Cytochrome bc_1 Complex†

Jason W. Cooley,‡ Tomoko Ohnishi,§ and Fevzi Daldal*,‡

Department of Biology, Plant Science Institute, and Department of Biochemistry and Biophysics, Johnson Research Foundation, University of Pennsylvania, Philadelphia, Pennsylvania 19104

Received March 29, 2005; Revised Manuscript Received June 9, 2005

ABSTRACT: Multiple instances of low-potential electron-transport pathway inhibitors that affect the structure of the cytochrome (cyt) bc_1 complex to varying degrees, ranging from changes in hydroquinone (QH_2) oxidation and cyt c_1 reduction kinetics to proteolytic accessibility of the hinge region of the iron−sulfur-containing subunit (Fe/S protein), have been reported. However, no instance has been documented of any ensuing change on the environment(s) of the [2Fe−2S] cluster. In this work, this issue was addressed in detail by taking advantage of the increased spectral and spatial resolution obtainable with orientation-dependent electron paramagnetic resonance (EPR) spectroscopic analysis of ordered membrane preparations. For the first time, perturbation of the low-potential electron-transport pathway by Q_i-site inhibitors or various mutations was shown to change the EPR spectra of both the cyt *b* hemes and the [2Fe−2S] cluster of the Fe/S protein. In particular, two interlinked effects of Q_i-site modifications on the Fe/S subunit, one changing the local environment of its [2Fe−2S] cluster and a second affecting the mobility of this subunit, are revealed. Remarkably, different inhibitors and mutations at or near the Q_i site induce these two effects differently, indicating that the events occurring at the Q_i site affect the global structure of the cyt bc_1. Furthermore, occupancy of discrete Q_i-site subdomains differently impede the location of the Fe/S protein at the Q_o site. These findings led us to propose that antimycin A and HQNO mimic the presence of QH_2 and Q at the Q_i site, respectively. Implications of these findings in respect to the Q_o−Q_i sites communications and to multiple turnovers of the cyt bc_1 are discussed.

The hydroquinone (QH_2):cytochrome (cyt) *c* oxidoreductase (cyt bc_1)[1] is an essential component of the mitochondrial and most bacterial respiratory electron-transport pathways (*1*). A sister complex, the cyt b_6f, is also a part of the photosynthetic electron-transport chains of the chloroplasts of higher plants and algae as well as of cyanobacteria (*2*). The bacterial cyt bc_1 are typically comprised of three catalytically active subunits that are the cyt *b* (with two *b*-type hemes b_H and b_L), the cyt c_1 (with a *c*-type heme), and the iron sulfur (Fe/S) protein with a high-potential [2Fe−2S] cluster (*1*). A comparison of the three-dimensional structures of the mitochondrial, chloroplast, and bacterial enzymes demonstrate that, despite the reduction of the subunit composition from the eukaryotic counterparts, the bacterial subunits have the same chemically active centers and also share the same interwoven homodimeric architecture (*3*, *4*). In one monomer, the amino terminal transmembrane (TM) anchor of the Fe/S protein subunit lies across the carboxyl-terminal TM helix of the cyt c_1 and the loop region connecting the *A* and *B* TM helices as well as a portion of the *A* TM helix of cyt *b*. Conversely, its membrane external domain bearing the [2Fe−2S] cluster oscillates between the cyt *b* and cyt c_1 subunits of the opposite monomer (*3*). The implications, if any, of such an elaborate architecture involving the Fe/S protein subunit being shared by both monomers is not yet understood.

It is currently thought that, during a complete catalytic turnover of the cyt bc_1, the Fe/S protein oxidizes in two rounds two QH_2 molecules to quinones (Q) at the QH_2 oxidation (Q_o) site of the enzyme on the positive (P) side of the energy-transducing membrane (*5*, *6*). After each oxidation event, the Fe/S protein leaves this special niche at the cyt *b* surface via a large-scale motion (i.e., macromovement) and transfers an electron to the cyt c_1 subunit. The cyt c_1 subsequently equilibrates with various soluble and membrane-attached electron-carrying *c*-type cytochromes recovering the fully oxidized state of the high-potential chain (*7*). Recent works proposed that the bifurcated QH_2 oxidation at the Q_o site might occur via either a "double-gated" mechanism with an extremely unstable semiquinone (SQ) intermediate or a

† This work was supported by NIH Grants R01 GM 38237 to F.D. and GM 30736 to T.O. and NIH F32 GM 65791 and AHA 0425515U fellowships to J.W.C.

* To whom correspondence should be addressed. Telephone: (215) 898-4394. Fax: (215) 898-8780. E-mail: fdaldal@sas.upenn.edu.

‡ Department of Biology, Plant Science Institute, University of Pennsylvania.

§ Department of Biochemistry and Biophysics, Johnson Research Foundation, University of Pennsylvania.

[1] Abbreviations: EPR, electron paramagnetic resonance; Fe/S, [2Fe−2S] cluster-containing protein; Q, quinone; cyt *b*, cytochrome *b*; QH_2, hydroquinone; cyt bc_1, hydroquinone:cytochrome (cyt) *c* oxidoreductase; HQNO, 2-heptyl-4-hydroxyquinoline *N*-oxide; NQNO, 2-nonyl-4-hydroxyquinoline *N*-oxide; Q_i, quinone reduction site; Q_o, hydroquinone oxidation site.

10.1021/bi050571+ CCC: $30.25
Published on Web 07/16/2005

"genuinely concerted" mechanism without invoking any SQ intermediates (*8*, *9*). Remarkably though, macromovement of the Fe/S protein is not required for the QH_2 oxidation per se at the Q_o site, although it is essential for its multiple turnover and the steady-state enzymatic activity of the cyt bc_1 (*10*, *11*). In any event, after each QH_2 oxidation, the remaining electron at the Q_o site is conveyed to cyt *b* hemes b_L and b_H then finally to a Q or SQ residing at the Q reduction (Q_i) site on the opposite negative (N) side of the membrane to regenerate a QH_2. Indeed, these QH_2/Q interconversions on the P and N sides of the membrane result in the net translocation of protons across the membrane and contribute to the formation of a proton motive force that is used to produce ATP (*5*).

Despite the complexity of the catalytic events that occur within the cyt bc_1, deleterious short circuit reactions that could decrease its energetic efficiency are extremely rare (*7*, *8*). For example, the yield of an apparent bypass reaction, whereby an oxidized Fe/S protein reoxidizes another QH_2 molecule at the Q_o site when the cyt *b* hemes are reduced, is very low (~1−2%) (*12*). Although electron-transfer rates and thermodynamic considerations can rationalize the catalytic safety of the cyt bc_1 during its initial Q_o-site turnover (*8*), the meaning of many experimental findings still remains unclear. For example, why, in the presence of antimycin A, electrons deposited to the heme b_H following a QH_2 oxidation at the Q_o site do not leak back to an oxidized cyt c_1 via the natural oscillation of the Fe/S protein (*13*−*15*). Similarly, it is not obvious why the macromovement of the extrinsic domain of the Fe/S protein, during which it interacts closely with the solvent-exposed cd_1, cd_2, and *ef* loops of cyt *b* (*10*, *16*, *17*), is required for multiple turnovers of the cyt bc_1. These and other observations often raise the issue of whether there exists in the cyt bc_1 some mechanism(s) preventing the occurrence of short circuits, especially during the onset of subsequent Q_o-site turnovers. A distinct possibility for such a mechanism might be to coordinate the Q_i site events tightly with the initiation of subsequent QH_2 oxidations at the Q_o site by cyt c_1 reoxidized [2Fe−2S] clusters. Several observations hinting at this possibility (*18*−*20*) and various proposals elaborating aspects of it (*20*) have been reported. We have also observed that various inhibitory events, which perturb electron transfer from the Q_o to the Q_i sites, affect thermolysin-mediated proteolytic cleavage of the hinge region of the Fe/S protein subunit (*21*). These inhibitory events include binding of antimycin A or HQNO, mutating specific Q_i-site residues or ligands of heme b_H, and imply that the steady-state positions of the Fe/S protein at the cyt *b* surface change accordingly. However, no direct information exists on how the interactions of Fe/S protein and its [2Fe−2S] cluster with the Q_o site or its occupants change in response to Q_i-site events.

In an attempt to gain evidence of Q_o−Q_i site interactions, we have undertaken a detailed study to monitor the behavior of the [2Fe−2S] cluster located at the P side of the membrane in response to various perturbations that occur at or near the Q_i site on the N side of the membrane using electron paramagnetic resonance (EPR) spectroscopy and native or mutant-derived ordered membranes. In this work, we present the first EPR spectral evidence that various events affecting the low-potential electron-transfer pathway of the cyt bc_1 also affect the steady-state interaction of the Fe/S protein with the Q_o-site occupants at the cyt *b* surface. Our findings indicate that both the nature of the molecule residing at the Q_i site as well as the absence of the cyt b_H cofactor influence the environment and the interactions of the Fe/S protein with the Q_o-site occupants. The implications of these findings on the steady-state turnover mechanism of the cyt bc_1 are discussed.

MATERIALS AND METHODS

Bacterial Strains and Growth Conditions. All *Rhodobacter capsulatus* strains were grown in mineral-peptone-yeast-extract-enriched media (MPYE) under semi-aerobic conditions in the dark at 35 °C, as described previously (*10*). The construction and growth phenotypes of the H212N and H217L, D, and R mutants have been described previously in refs *8* and *22*, respectively.

Preparation and Spectroscopic Analysis of Ordered Membrane Samples. Chromatophore membrane isolation was carried out as described previously in ref *23*. Ordered membrane sample preparation was modified from those outlined in refs *24* and *25* and described in detail in ref *26*. Chemical depletion of Q from chromatophore membranes (<1 Q per reaction center) was carried out as outlined in ref *27*. Using membrane samples, EPR spectra were recorded between angles of 0−180° from the magnetic field vector using 5° rotational intervals for 0−120° and 10° steps thereafter. EPR spectroscopy was carried out at sample temperatures of 10 or 20 K on a Bruker ESP 300E spectrometer (Bruker Biosciences), fitted with an Oxford instruments ESR-9 helium cryostat (Oxford Instrumentation Inc.). Additional spectrometer settings were as indicated in the captions of the figures. For orientation-dependent spectral acquisition, a goniometer of homemade design, sufficient for consistent reproduction of angular values (±2.5°), was utilized. Stock solutions of antimycin A, HQNO (Sigma−Aldrich Inc.), or stigmatellin (Fluka Inc.) were prepared in dimethyl sulfoxide and added at desired concentrations to the membrane samples prior to drying or freezing. Except otherwise noted, concentrations of antimycin A, HQNO, and stigmatellin were 10, 30, and 5 μM per ~30 mg/mL total chromatophore membrane proteins, respectively. Chemical reduction of the samples was achieved by addition of Na−ascorbate (Sigma−Aldrich Inc.) to 5 mM final concentrations. EPR samples were stored in liquid N_2 until spectra were recorded.

RESULTS

Antimycin A and HQNO Binding to the Q_i Site Are Sensed throughout the Native or Mutant Cyt bc_1 Lacking an Intact Low-Potential Electron-Transfer Chain. As a prelude to a detailed probing of the interactions between the Q_o and Q_i sites, we initially examined if the binding of Q_i-site inhibitors antimycin A or HQNO to *R. capsulatus* native and selected mutant cyt bc_1 affected the EPR spectra of the cyt *b* hemes. Addition to the wild-type membrane preparations of either of these inhibitors conveyed small but significant spectral alterations of either the shapes or positions of the cyt b_H, as described previously in ref *28*, and b_L hemes EPR g_z transitions (Figure 1).

A small but reproducible shift in the g_z position of the b_L heme, from 3.783 in the untreated native membranes to 3.779

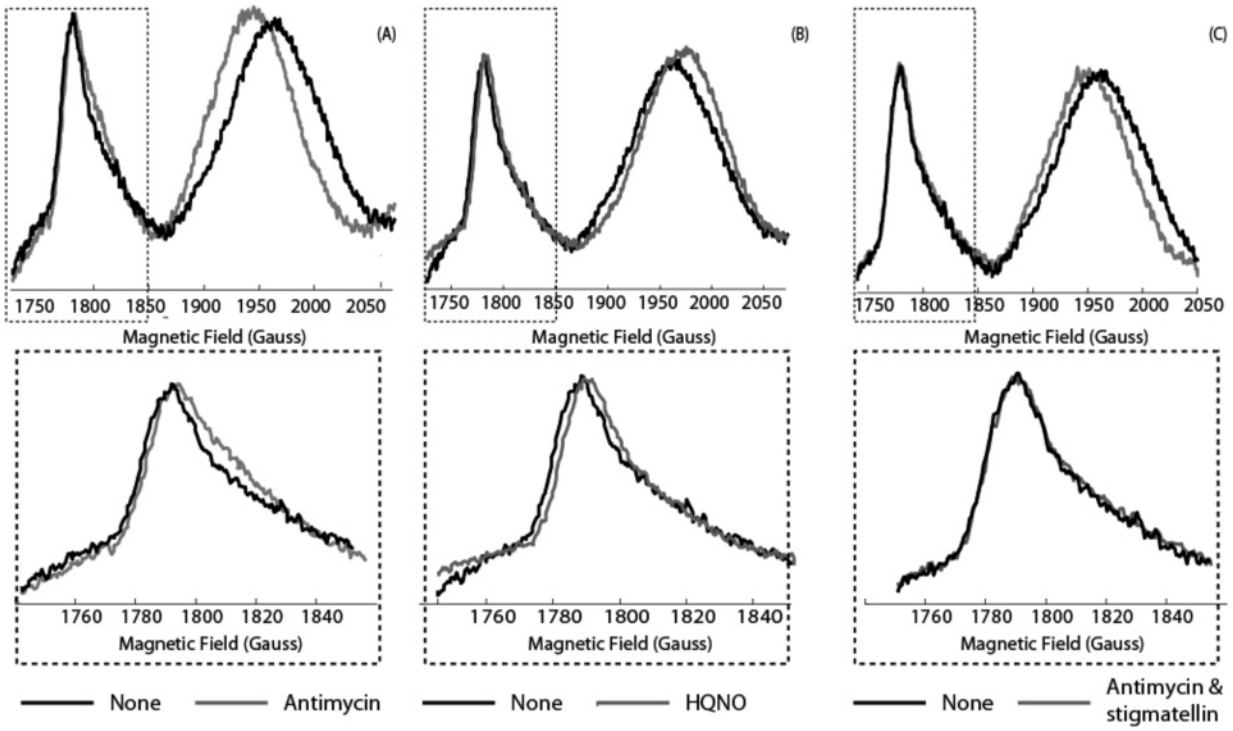

FIGURE 1: EPR spectra of the wild-type cyt *b* heme g_z transitions in the presence or absence of Q_i-site inhibitors. Nonordered membranes were prepared in the presence (gray traces) or absence (black traces) of antimycin A (A), HQNO (B), and antimycin + stigmatellin (C). For clarity, the g_z transition of the b_L heme (boxed) is shown at a higher magnification in the lower portion of each panel. EPR spectra of ascorbate (5 mM) reduced frozen membrane solutions were recorded at 10 K, 9.443 GHz microwave frequencies, and modulation amplitudes of 10 G.

or 3.775 upon addition of antimycin or HQNO, respectively, was seen. While the magnitudes of the peak position shifts were small, the spectral maxima were sharp and well-defined, allowing accurate assignments. Moreover, mutants lacking either the b_H heme iron-liganding histidine (H212N) or the Q_i-site Q-liganding histidine (H217R and L) residues also caused pronounced changes in the cyt b_L heme EPR g_z transition and line shape even in the absence of any inhibitor ($g_z = 3.790$ for H212N or 3.789 for H217R) as compared to those seen in the wild-type cyt bc_1 ($g_z = 3.783$) (Figure 2). The data indicated that changes induced by inhibitor binding occurring on the N side of the membrane are propagated throughout the protein complex to its P side.

Addition of Antimycin A to Ordered Membrane Samples Alters the EPR Spectral Shape of the [2Fe−2S] Cluster of the Cyt bc_1. In contrast to what was observed with the cyt b_H and b_L hemes, addition of either antimycin A or HQNO to membranes exhibited no discernible effect on the EPR transitions of the [2Fe−2S] cluster in nonordered (or powder) sample EPR spectra (Figures 3 and 4), as has been described earlier (*26*). Unlike the tensor-averaged powder sample EPR spectra, use of ordered membrane samples increases both the spectral resolution of a given transition in the EPR spectrum and also yields specific information about the relative orientation (and the relative numbers of different orientations) of a metal cluster in a given sample. Therefore, we also examined ordered membrane samples from wild-type *R. capsulatus* membranes to probe the effects of Q_i-site inhibitors on the interactions of the [2Fe−2S] cluster of the Fe−S protein with the Q_o site of the cyt bc_1. Unlike what was seen in Figure 3A, upon antimycin A addition, EPR spectra of similarly treated ordered membrane samples exhibited marked shifts at both the g_x and g_y transitions (Figure 3B and Table 1).

Moreover, spectral line shape broadening and decreased orientation dependence, as evidenced by plotting the amplitudes of the g_x and g_y transitions as a function of the angle of the membrane versus the magnetic field vector, were also observed (Figure 3C). Use of ordered membrane preparations of comparable quality was ensured by monitoring the g_z transition of the immobile cyt b_H heme (Figure 3D). Previously, broadening of the g_x transition in ordered membranes has been associated with increased mobility of the Fe/S protein, as induced by the class II Q_o site inhibitor myxothiazol or by chemical depletion of Q from chromatophore membranes (*26*). In these cases, the total amount of the Fe/S protein residing at the cyt *b* surface was diminished, and the EPR g_y transition of the [2Fe−2S] cluster shifted to slightly lower magnetic field positions. Furthermore, in similarly ordered membranes, increased mobility of the Fe/S protein was also accompanied by a diminished orientation dependence of the [2Fe−2S] cluster spectrum (*26*). The similarities of these observations to the data obtained by addition of antimycin A suggested that the membrane embedded cyt bc_1 has an increased mobility of the Fe/S protein subunit. Thus, in the presence of this inhibitor, the Fe/S subunit appeared to move more freely and, consequently, interacted less with the Q_o-site occupants. However, because addition of antimycin A does not decrease the redox midpoint potential of the [2Fe−2S] cluster, determined by the titration of its g_y signal (data not shown), the head domain of the Fe/S protein still lies probably at the cyt *b* surface near its *ef* loop (*29*).

HQNO Binding at the Q_i Site Also Alters the Steady-State [2Fe−2S] Cluster Environment. HQNO also binds at the Q_i site of the cyt bc_1 and inhibits the enzyme activity in a manner similar to antimycin A (*30*, *31*). However, the interactions of HQNO with the cyt *b* are different from those observed

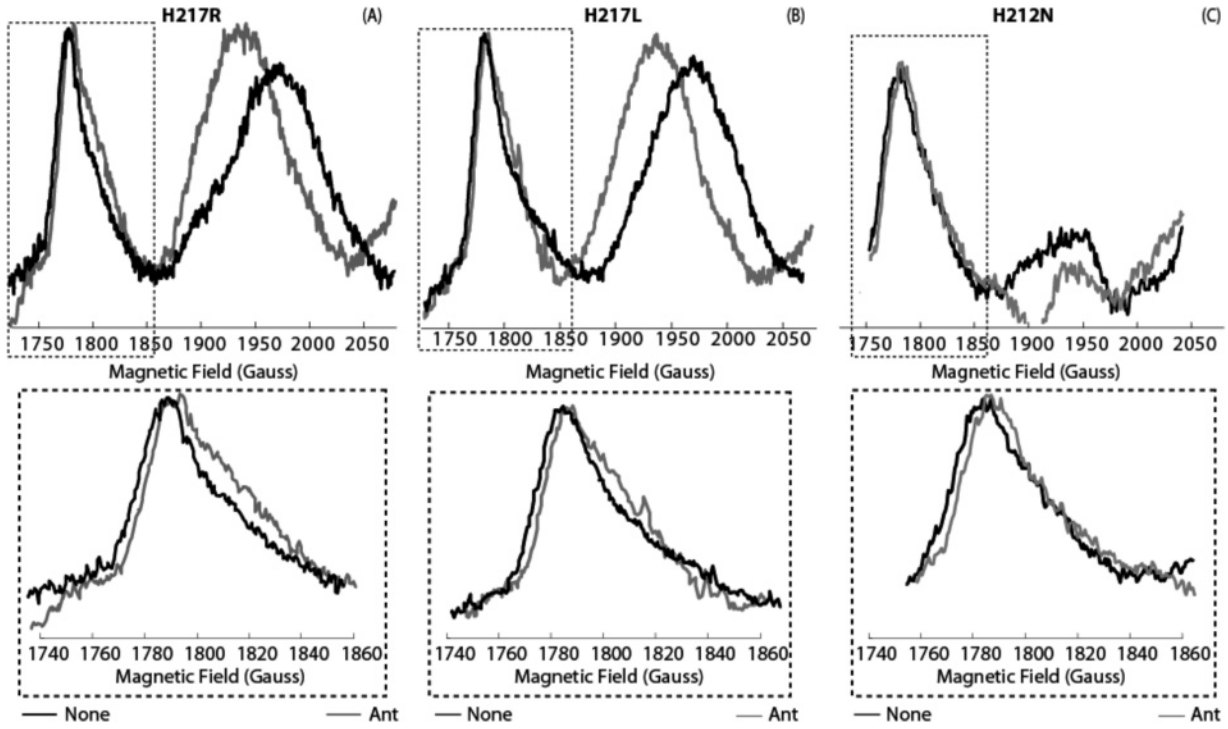

FIGURE 2: EPR spectra of various low-potential chain mutants cyt *b* heme g_z transitions in the presence or absence of antimycin A. Mutants H217R (A), H217L (B), and H212N (C) derived nonordered membranes were prepared in the presence (gray traces) or absence (black traces) of antimycin A. For clarity, the g_z transition of the cyt b_L heme (boxed) is shown at a higher magnification in the lower portion of each panel. Chemical reduction and spectrometer settings were as described in Figure 1. Note that because the H212N mutant lacks the cyt b_H heme, no corresponding g_z transition is observed

with antimycin A as indicated by both its lower binding affinity (*32*) and the comparison of the crystal structures containing NQNO (*33*). NQNO is a structurally similar molecule to HQNO and antimycin A. Complementary to what was observed with antimycin A, addition of 30 μM HQNO also affected the EPR spectrum of the [2Fe−2S] cluster in ordered membranes (Figure 4A).

Remarkably though, the effects induced by HQNO were distinct from those seen with antimycin A, in that the changes observed were limited predominantly to the portion of the spectra associated with the g_x transition. When compared with untreated ordered EPR spectra, the g_x transition was broadened by over 35 G at its maximum amplitude, while its position in the magnetic field sweep was changed to only a slightly higher value (Table 1). In addition, unlike that seen with antimycin A, the orientation dependence of the spectra was unchanged in the presence of HQNO when compared to those derived from untreated native samples (Figure 4B). Thus, while binding of HQNO to the cyt bc_1 also induced a change in the environment of the [2Fe−2S] cluster at the Q_o site, it has done so without increasing the tendency of the Fe/S protein to move more freely at or away from the cyt *b* surface.

The [2Fe−2S] Cluster Environment in Q-Depleted Membranes Is Modified by the Tight Binding Q_o-Site Inhibitor Stigmatellin but Not by Antimycin A or HQNO. The EPR spectra of the [2Fe−2S] cluster of the wild-type cyt bc_1 containing ordered membranes that are chemically depleted of Q are broadened, and the positions of the g_x and g_y transitions are shifted up- and downfield, respectively (Table 1). Additionally, these EPR spectra lack significant orientation dependence upon rotation of the sample in the spectrometer (Figure 5).

To ensure that the effects on the [2Fe−2S] cluster EPR spectra seen with antimycin A and HQNO are not due to their binding to the Q_o site, either of these Q_i-site inhibitors alone or in combination with stigmatellin were added to Q-depleted membranes. Under the experimental conditions used here, neither HQNO nor antimycin A had any significant effect on the line shape or orientation dependence of the [2Fe−2S] cluster in the absence of Q. Moreover, in each case, subsequent addition of stigmatellin yielded spectra similar to those seen with this Q_o-site inhibitor when nonchemically treated native membranes were used (Figure 5). These data imply that neither of the Q_i-site inhibitors directly interacts with the [2Fe−2S] cluster nor does either inhibitor grossly alter the binding and interactions of stigmatellin with the Q_o site.

Mutations that Affect the Q_i-Site Semiquinone Radical Anion Stability Alter the [2Fe−2S] Cluster EPR Spectrum. The amino acid residue H217 of cyt *b* is thought to be involved in liganding Q at the Q_i site (*22*, *33*, *34*). Previous characterizations of mutants where this residue were substituted with leucine, aspartate, and arginine (H217L, D, and R, respectively) indicated that the ability to form a stable SQ at the Q_i site was severely diminished (*22*). Although the EPR spectra of the [2Fe−2S] clusters of the mutant cyt bc_1 obtained using powder samples were similar to those seen using wild-type membranes (Figure 6A), when ordered membranes were examined the g_x transitions of the [2Fe−2S] clusters in different mutants exhibited various extents of broadening (Figure 6B).

The characteristic $g_x = 1.80$ signal, indicative of the [2Fe−2S] cluster interacting with a Q residing at the Q_o site, was almost entirely lost (perhaps with the exception of the H217L mutant), and a new transition maximum localized at $g =$

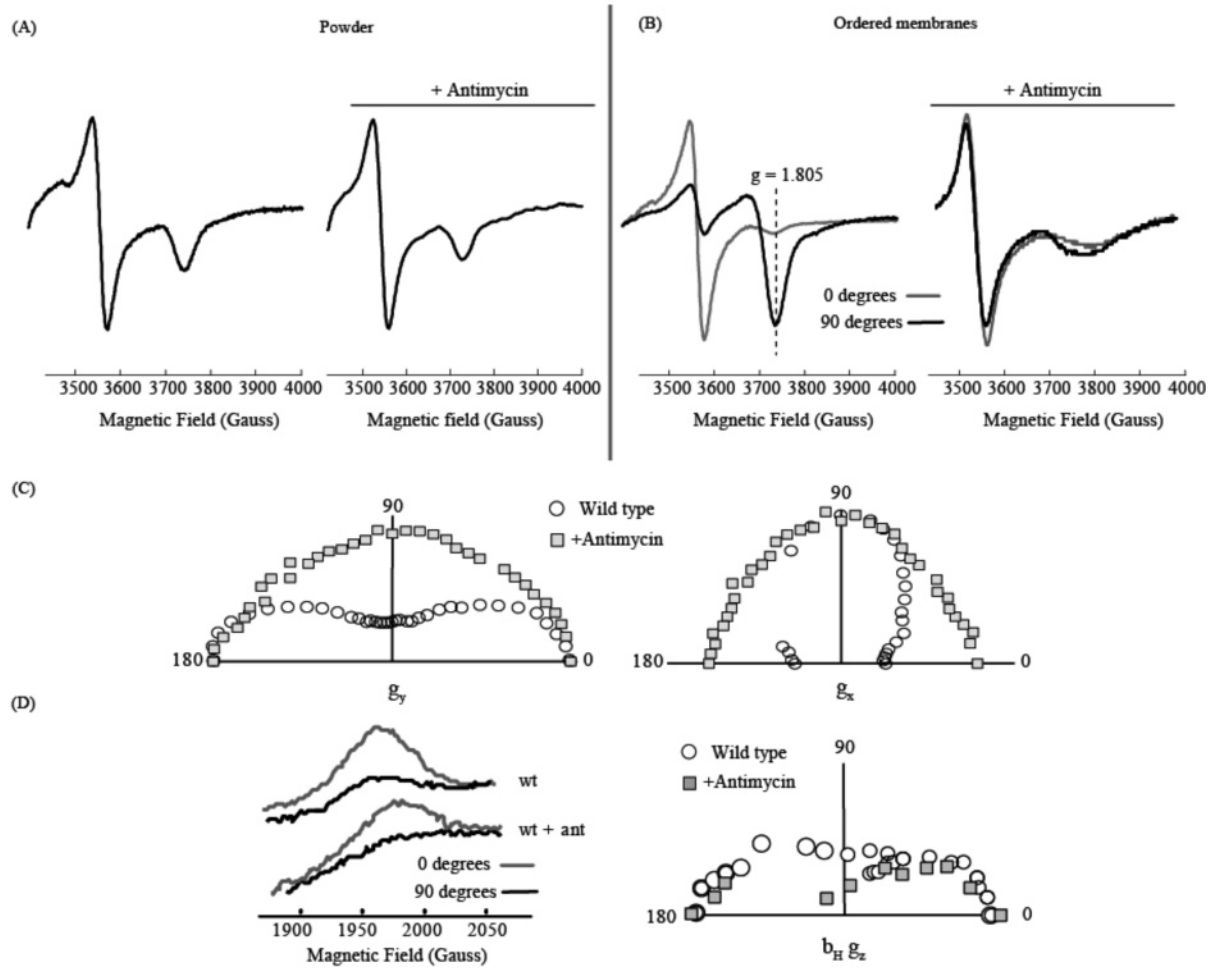

FIGURE 3: Orientation-dependent EPR spectra of the [2Fe−2S] cluster of the Fe/S protein using ordered wild-type membranes treated with antimycin A. Wild-type nonordered (A) and ordered (B) membranes were prepared in the presence (right portion of panel) or absence (left portion of panel) of antimycin A (10 μM). For ordered membrane samples, only the spectra acquired at orientation versus the magnetic field where the g_y (gray traces) or g_x (black traces) transition amplitudes were maximal are shown. Polar plots of the g_y (C, left portion) and g_x (C, right portion) transition amplitudes as a function of the rotation of the membrane plane versus the magnetic field are displayed to illustrate the change in orientation dependence before (white circles) and after (gray boxes) inhibitor addition. Maximal (black) and minimal (gray) amplitude containing spectra of the membrane embedded cyt b_H heme g_z transitions and the resulting polar plots of the dependence of these amplitudes as a function of the sample rotation in the spectrometer cavity before (white circles) and after antimycin addition (gray triangles) have also been illustrated to show the similarity of membrane layering in each sample (D, left and right, respectively). Membranes were prepared as described in the Materials and Methods, and the EPR spectra were recorded at 20 K, 9.443 GHz microwave frequencies, with modulation amplitudes of 12 G.

1.79 appeared (Figure 6B and Table 1). Moreover, the position of the g_y transitions seen with the H217R and L ordered membranes were also shifted to higher magnetic field values, $g_y = 1.898$ versus $g_y = 1.895$ seen with wild-type samples (Figure 6B and Table 1). Even in the H217D mutant that has the most favorable formation of SQ at the Q_i site among the strains tested, a smaller (though still substantial) shift of the g_y transition to 1.897 was observed (Figure 6B and Table 1). Finally, the orientation dependence of the EPR spectra of ordered membrane samples of these mutants was affected more than that induced with HQNO but less than that mediated by addition of antimycin A to the native enzyme (Figure 6C). Because reoxidation of reduced cyt b_H is defective as evidenced by perturbations of the antimycin A sensitive SQ EPR signal at the Q_i site in the H217L, D, and R substitutions (*22*), the EPR data indicated that even partial inhibitions of the low-potential pathway were sufficient to change the environment of the [2Fe−2S] cluster at the Q_o site in the cyt bc_1.

Elimination of the Cyt b High-Potential Heme b_H Also Affects the Interactions of the [2Fe−2S] Cluster of the Fe/S Protein with the Q_o Site. Elimination of the cyt *b* high-potential heme b_H by replacing its axial-liganding histidine at position 212 with an asparagine (H212N) yields a mutant cyt bc_1 that is both stable and able to oxidize QH_2 at the Q_o site (*8*, *22*, *35*). As in the case of the wild-type cyt bc_1 or its H217R, L, and D mutant derivatives, using powder samples, the [2Fe−2S] cluster EPR spectrum of the H212 mutant enzyme was virtually unchanged from the native enzyme (Figure 7A). On the other hand, it was again possible to discern changes in these EPR spectra using ordered membrane samples (Figure 7B).

Similar to the other low-potential pathway inhibited cyt bc_1 mutants, the g_x transition broadened significantly, but unlike the H217 derivatives, this transition retained its 1.80 value. Despite this retention, the $g = 1.8$ transition appeared diminished because a broader spectrum centered at a lower *g* value grew in beneath it (Figure 7B). In the EPR spectra

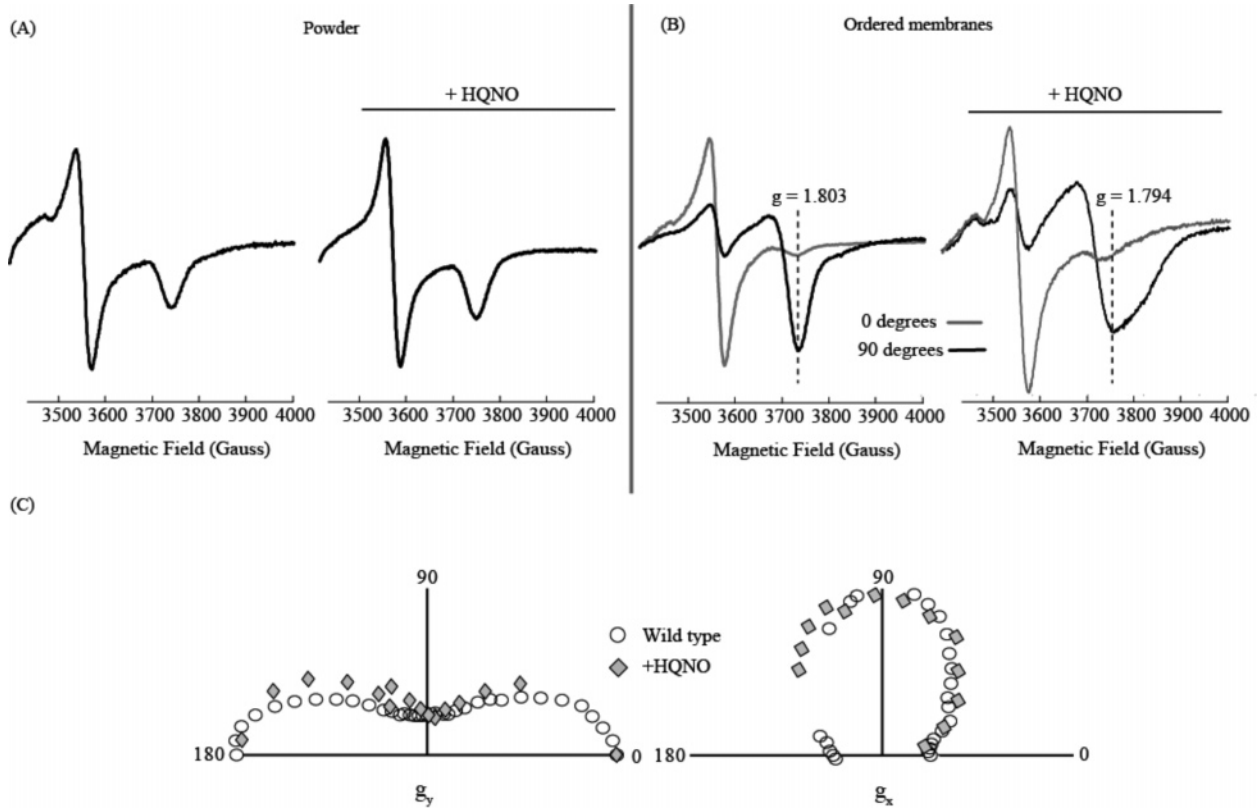

FIGURE 4: Orientation-dependent EPR spectra of the [2Fe−2S] cluster of the Fe/S protein using ordered wild-type membranes treated with HQNO. Wild-type nonordered (A) and ordered (B) membranes were prepared in the presence (right portion of panel) or absence (left portion of panel) of HQNO (30 μM). As in Figure 3, only the spectra acquired at orientation versus the magnetic field where the g_y (gray traces) or g_x (black traces) transition amplitudes were maximal are shown for ordered membrane samples. Polar plots of the g_y (C, left portion) and g_x (C, right portion) transition amplitudes as a function of the rotation of the membrane plane versus the magnetic field are displayed to illustrate the change in orientation dependence before (white circles) and after (gray boxes) inhibitor addition. Membranes were prepared as described in the Materials and Methods, and the EPR spectrometer settings were essentially the same as those described in Figure 3.

Table 1: EPR *g* Transition Positions and Spectral Widths from Various Ordered Membrane Samples

	transition position (g)		transition width (Gauss)	
	g_x	g_y	g_x	g_y
wild type				
no inhibitor	1.804	1.895	161	31
+stigmatellin	1.782	1.893	170	32
+myxothiazol	1.773	1.902	208	48
+antimycin A	1.776	1.902	207	46
+HQNO	1.794	1.893	226	38
−Q[a]	1.765	1.900	∼220	51
+antimycin A (+stigmatellin)	1.765(1.783)	1.900(1.890)	∼220(168)	51(36)
+HQNO (+stigmatellin)	1.765(1.783)	1.900(1.890)	∼220(181)	51(39)
H212N mutant	1.803	1.899	200	48
+antimycin A	1.799	1.903	209	50
H217L mutant	1.802	1.902	208	52
+antimycin A	1.774	1.903	206	49
+stigmatellin	1.782	1.893	173	32
H217D mutant	1.795	1.902	227	55
+antimycin A	1.778	1.903	197	48
H217R mutant	1.790	1.901	206	52
+antimycin A	1.775	1.904	206	50
+HQNO	1.783	1.897	225	39

[a] Values in parentheses refer to those obtained in the presence of stigmatellin.

of the H212N mutant, the g_y position also shifted to a lower magnetic field position (i.e., higher *g* value) at its maximal amplitude, and this shift was intermediate between what has been observed with the native cyt bc_1 and with myxothiazol-inhibited or Q-depleted enzyme (Table 1). Last, the H212N samples also exhibited a diminished degree of orientation dependence of the EPR spectra of the [2Fe−2S] cluster in similarly ordered membrane samples (Figure 7C). Overall, the data indicated that elimination of the cyt b_H heme also changed the environment of the [2Fe−2S] cluster at the Q_o site, but the mobility of the Fe/S protein at the cyt *b* surface was intermediate between untreated or HQNO-treated versus antimycin A-treated samples.

The [2Fe−2S] Cluster EPR Spectra of Mutants with a Defective Low-Potential Pathway Are Also Affected by Antimycin A. Antimycin A appeared unique in inducing a

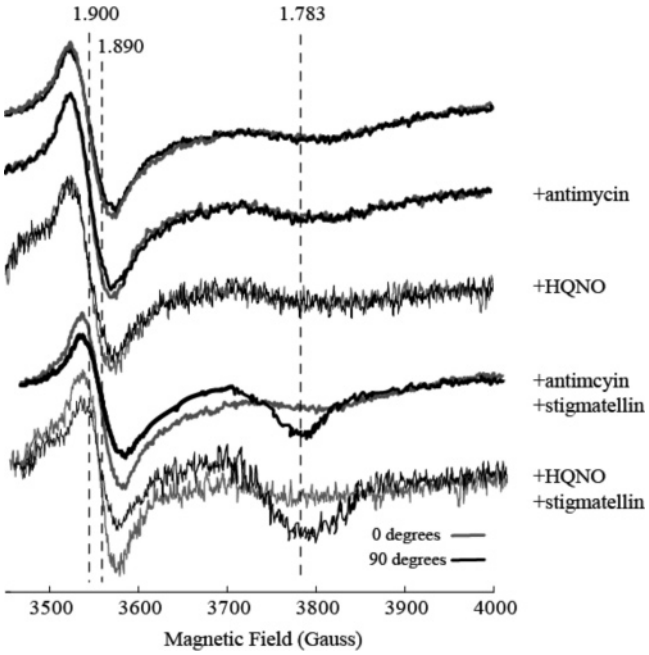

FIGURE 5: Orientation-dependent EPR spectra of the [2Fe−2S] cluster of the Fe/S protein using ordered Q-depleted wild-type membranes treated with Q_i- and Q_o-site inhibitors. Wild-type ordered membranes containing <1 Q per reaction center were prepared in the absence or presence of antimycin A, HQNO, antimycin A + stigmatellin, or HQNO + stigmatellin with final concentrations of antimycin A, HQNO, and stigmatellin of 10, 30, and 10 μM, respectively. Only the spectra acquired at orientations versus the magnetic field where the g_y (gray traces) or g_x (black traces) transition amplitudes were maximal are shown. Membranes were prepared as described in the Materials and Methods, and the EPR spectra were recorded at 20 K, 9.443 GHz microwave frequencies, with modulation amplitudes of 12 G.

complete lack of the orientation dependence of the [2Fe−2S] cluster EPR spectrum among the various means of inhibition of the low-potential pathway that were tested in this work. This observation suggested that, in addition to or instead of a mere inhibition of electron transfer, other components acting more specifically might also be responsible for the increased mobility of the Fe/S protein at the Q_o site. Therefore, we also examined the effects of adding antimycin A to mutants that are already defective for the function of the low-potential pathway, such as the H217L, D, and R or H212N substitutions. Remarkably, addition of this inhibitor to the membrane samples derived from H212N or H217R induced a nearly complete lack of orientation dependence of the [2Fe−2S] cluster EPR spectrum (Figure 8, and H217L and D not shown). In addition, the EPR spectra of these mutants treated with antimycin A had their g_y and g_x transitions shifted to higher and lower magnetic field g values, respectively, as listed in Table 1. Upon subsequent addition of stigmatellin, the EPR spectra became indistinguishable from those seen in the presence of stigmatellin alone (see, e.g., Table 1 for H217L), indicating that the antimycin A-induced changes seen in the mutants defective in the low-potential chain could be nullified by a tight binding Q_o-site inhibitor such as stigmatellin. This is similar to that seen with a wild-type cyt bc_1 (not shown but comparable to the cyt *b* EPR spectra in Figure 1). On the other hand, HQNO addition to the membranes derived from the H217R mutant for example did not affect the orientation dependence of the EPR spectra of the [2Fe−2S] cluster of the Fe/S protein (Figure 8), also similar to that seen with the wild-type cyt bc_1. Equally similar to wild-type cyt bc_1 samples, addition of HQNO to membranes derived from the H217R mutant dramatically changed the EPR spectral line shape in the portion correlative with the g_x transition. Thus, the finding that antimycin A acted in a similar fashion both in the wild type and in various cyt bc_1 mutants with defective low-potential chains clearly indicated that the drastic increase of the mobility of the Fe/S protein head domain appeared to be an intrinsic property of the binding of this inhibitor to the Q_i site and not due to either a perturbation of the low-potential chain or a change in the general occupancy of the Q_i site per se.

DISCUSSION

We have previously reported the monitoring of gross changes in the equilibrium location of the Fe/S protein in the cyt bc_1 as a function of inhibitors and single-site mutations by the utilization of thermolysin-mediated cleavage (*21*). With the native enzyme, this proteolytic cleavage was completely inhibited or unchanged by the addition of the Q_o-site inhibitors stigmatellin or myxothiazol, respectively, and surprisingly was enhanced by the Q_i-site inhibitor antimycin A. Similarly, enhanced proteolysis of the extrinsic domain of the Fe/S protein in isolated proteins or partially solubilized membrane preparations was also observed with cyt *b* H212N and H217L, D, and R mutants, which have defective low-potential chains. Enhancement of cleavage by antimycin A was not additive to the levels of proteolysis with the mutant enzymes, because they already exhibited cleavage levels significantly above that of the wild type prior to inhibitor addition (*21*). Structural data correlating the specific positions of the [2Fe−2S] cluster of the Fe/S protein in the presence of inhibitors (*36*) suggested that the extent of the cleavage reaction reflected the position of the extrinsic domain of the Fe/S subunit in the wild-type and mutant enzymes (*21*). However, because the proteolysis occurred at the hinge region of the Fe/S protein, these experiments provided no direct data about the location of the [2Fe−2S] cluster in the cyt bc_1. Thus, EPR spectroscopy was undertaken to more directly monitor the effects of various Q_i inhibitors on modifying the location of the [2Fe−2S] cluster at the Q_o site.

EPR spectra of cyt bc_1 [2Fe−2S] clusters in powder samples exhibited no obvious changes upon addition of antimycin A or HQNO in our hands (Figures 3 and 4). However, both antimycin A and HQNO affected not only the EPR transitions corresponding to the Q_i site adjacent cyt b_H heme (*33*, *36*) but also those of the cyt b_L heme on the opposite side of the membrane. Indeed, in line with our observations, long-range effects induced by Q_o- and Q_i-site inhibitors or Q_i-site mutations (*22*) on the local environment of the cyt *b* hemes have been detected previously using conventional optical spectroscopies (*32*, *37*).

EPR Spectroscopy of Ordered Membrane Samples Reveals that Q_i-Site Inhibitors or Low-Potential Chain Mutations Affect the Interactions of the [2Fe−2S] Cluster with the Q_o Site. Encouraged by the ability of EPR spectroscopy to reveal both local and distant structural effects of both inhibitor binding and mutagenesis on the cyt *b*, we have taken advantage of the increased spectral and spatial resolution

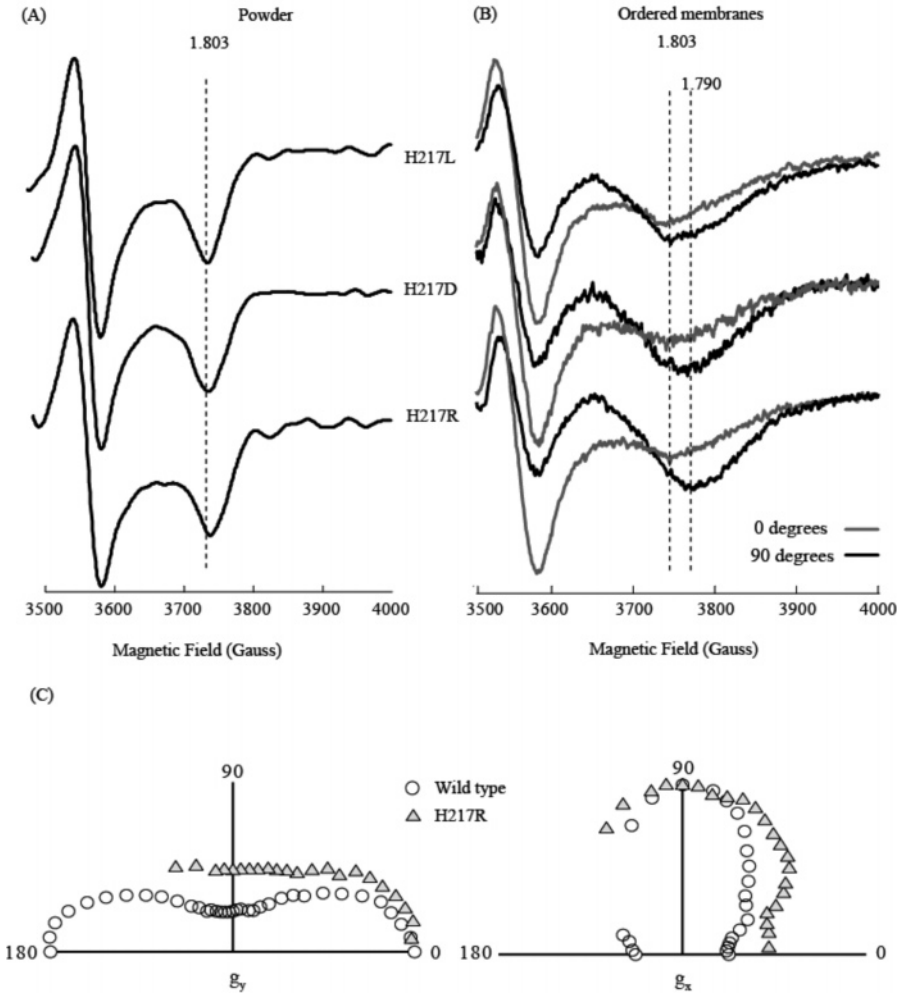

FIGURE 6: Orientation-dependent EPR spectra of the [2Fe−2S] cluster of the Fe/S protein using ordered membranes from the low-potential chain defective H217L, D, and R mutants. EPR spectra of the H217L, D, and R mutants (upper, middle, and lower, respectively) using nonordered (A) and ordered (B) membranes are shown. The characteristic wild-type $g = 1.8$ g_x transition maximum and the new maximum $g = 1.79$ are specified with dotted vertical lines. Polar plots similar to those presented in Figures 3 and 4 are shown in C to illustrate the diminished orientation dependence of the EPR spectra of the H217R mutant (gray triangles) as compared to similarly untreated wild-type (white circles) membrane preparations. Spectrometer settings were as described in Figure 3.

associated with oriented EPR analysis of ordered membrane samples to probe the possible effects related to the [2Fe−2S] cluster of the Fe/S protein at the Q_o site. The data provided direct evidence that binding of the Q_i-site inhibitors on the N side of the membrane or mutations severing the low-potential chain of the cyt bc_1 affected the environment of the [2Fe−2S] cluster of the Fe/S protein at the Q_o site on the opposite P side of the membrane. Remarkably, we have observed for the first time a variety of changes in the EPR spectra of the [2Fe−2S] cluster of the Fe/S protein upon addition of antimycin A or HQNO to both the wild type and specific mutants (Table 1).

Specifically, we have detected two types of changes associated with the changing occupancy or structure of the Q_i site on the [2Fe−2S] cluster EPR spectra. The first set of changes, exemplified by those complexes with HQNO bound at the Q_i site, modified only the line shape of the EPR spectra. While NQNO (and presumably HQNO) is thought to also bind at the Q_o site of the cyt bc_1 in a manner similar to stigmatellin (*33*), no evidence was seen that it does so under the conditions used here. In fact, no change in the [2Fe−2S] cluster EPR line shape was detected when HQNO was added to Q-depleted membranes (Figure 5), indicating that the changes seen in the [2Fe−2S] cluster environment are mediated by the binding of this inhibitor at the Q_i site. Additionally, the HQNO-mediated changes to the [2Fe−2S] cluster EPR spectrum of ordered membrane samples depended upon the presence of Q at the Q_o site. The second set of changes also exhibit similarly dramatic modifications of the line shape of the EPR spectra, but in these cases, the orientation dependence of these spectra were also perturbed. Orientation dependence of the EPR spectra of ordered membrane samples can provide important information about the mobility of the Fe/S protein extrinsic domain. Previously, a decrease of the orientation dependence of the EPR spectra, using similarly oriented membrane samples, was correlated with the increased mobility of the Fe/S protein extrinsic domain away from the cyt *b* surface (*26*). Remarkably, although both antimycin A and HQNO changed the environment of the [2Fe−2S] cluster at the Q_o site, only addition of antimycin A decreased the orientation dependence of the EPR spectra. Thus, even though both of these inhibitors abolish cyt *b* reoxidation upon its reduction via the Q_o-site turnover, their effects on the interactions of the [2Fe−2S] cluster with

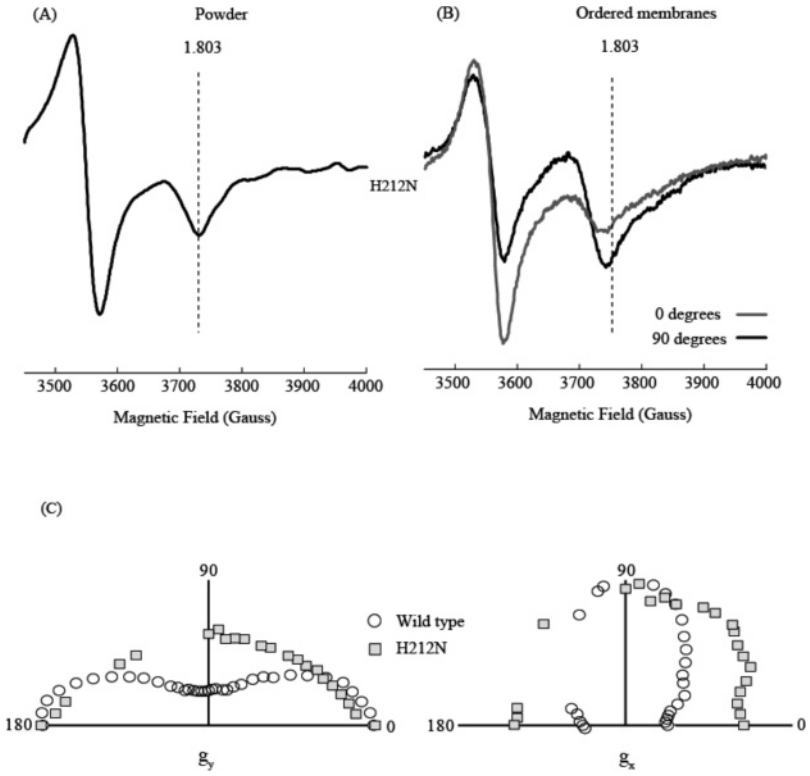

FIGURE 7: Orientation-dependent EPR spectra of the [2Fe−2S] cluster of the Fe/S protein using ordered membranes from a cyt b_H hemeless mutant H212N. EPR spectra of the H212N mutant using nonordered (A) and ordered (B) membranes are shown. The characteristic wild-type $g = 1.8$ g_x transition maximum is specified with a dotted line in each panel. Polar plots similar to those presented in Figures 3−5 are shown in C to illustrate the diminished orientation dependence of the H212N mutant (gray squares) as compared to similarly untreated wild-type (white circles) membrane preparations. Spectrometer settings were as described in Figure 3.

the Q_o site differ significantly, as if the individual inhibitor-bound states were mimicking discrete steps or intermediates of Q_i-site catalysis.

Various mutants with inherently defective low-potential chains of the cyt bc_1, such as H212N lacking the cyt b_H or the H217L, D, and R modified in the stabilization of the SQ at the Q_i site, were also examined. In the case of the H217R mutant, untreated membrane samples already had a [2Fe−2S] cluster EPR line shape lacking a clear $g_x = 1.8$ transition and a somewhat decreased orientation dependence. When treated with antimycin A, they looked similar to those obtained using the soluble portion of the Fe/S protein (*38*) or to the ordered samples containing native cyt bc_1 either treated with myxothiazol or chemically Q depleted (*26*). Conversely, the orientation dependence of these spectra was still visible with samples treated with HQNO. On the other hand, in the case of the H212N mutant samples, a significant portion of the $g_x = 1.8$ transition, thought to be indicative of the Fe/S ↔ Q interaction, was still detectable in the absence of antimycin A. After antimycin A treatment, this signal broadened in the high field portion of the g_x transition and the orientation dependence was diminished but not lost completely. This is in contrast to the similarly treated H217R mutant cyt bc_1. Apparently, mutations with a defective low-potential chain already have a partially increased mobility of the Fe/S protein even in the absence of the Q_i inhibitors, and addition of antimycin A but not of HQNO further diminished the orientation dependence of the [2Fe−2S] cluster EPR spectra. Because the effects induced by the Q_i-site mutations and by antimycin A were not synergistic, the Fe/S protein appears to have reached a maximum mobility in the presence of antimycin A. However, the increased mobility does not appear to encompass a large displacement from the niche near the cyt *b* surface, because otherwise one would have observed a decreased redox midpoint potential for the [2Fe−2S] cluster of the Fe/S protein, as seen with myxothiazol addition (*29*) (data not shown). Remarkably, the effects of Q_i-site inhibitors on the interaction of the [2Fe−2S] cluster with the Q_o site are not reflective of redox-related changes within the components of the low-potential pathway. This observation indicates that the physical interaction of the molecule at the Q_i site and its chemical nature are more directly correlated to the two different types of effects seen with the [2F−2S] cluster.

Structural Basis of the Differential Effects of Antimycin A versus HQNO on the Interactions of the [2Fe−2S] Cluster of the Fe/S Protein with the Q_o Site. Examination of the available three-dimensional structures of the cyt bc_1 with Q_i-site occupants indicate that, while both antimycin A and NQNO (a structural analogue of HQNO) displace Q from the Q_i site, they use an overlapping but nonidentical set of residues as binding ligands (upper and middle panels of Figure 9). Q_i-site coordination of antimycin A involves the amino acids K251 and D252 as well as H217 (*R. capsulatus* numbering) located in the TM helices *D* and *E*, respectively. Additionally, van der Waals interactions with I49 and A52 of helix *A* and the heme b_H propionates of the cyt *b* subunit are observed in the various solved structures with antimycin A present (*33*, *36*). The *D* helix, in addition to coordinating the Q_i-site inhibitor, also contains the H198 and H212 (*R. capsulatus* numbering) residues that are the axial ligands of the Fe atoms of the cyt b_L and b_H hemes, respectively. The

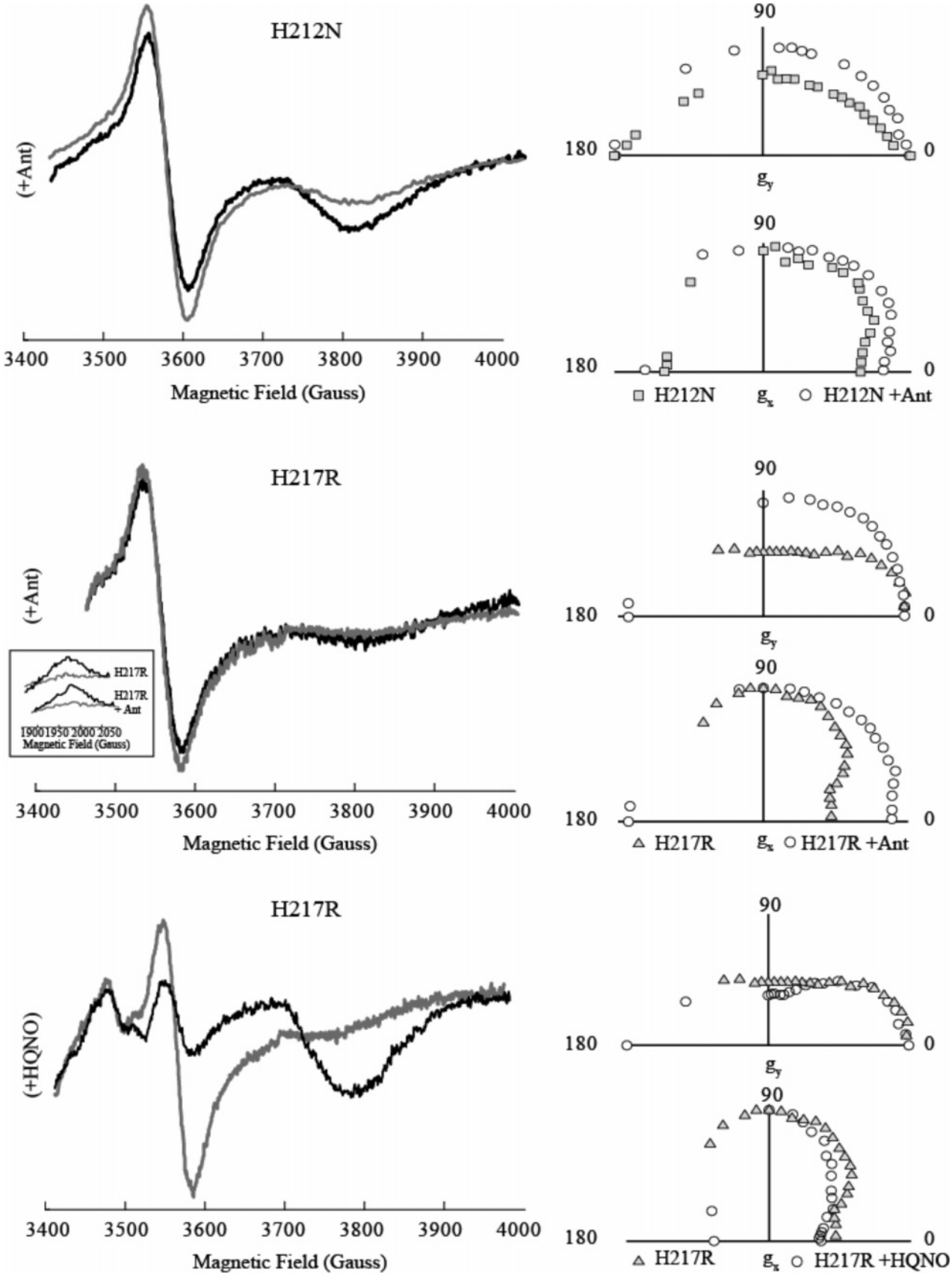

FIGURE 8: Orientation-dependent EPR spectra of the [2Fe−2S] cluster of the Fe−S protein using ordered mutant membranes from low-potential chain defective mutants treated with Q_i-site inhibitors. EPR spectra of the H212N and H217R mutants in the presence of antimycin A (10 μM) (upper and middle panel, respectively) and H217R mutant in the presence of HQNO (30 μM) (lower panel) obtained using ordered membranes are shown on the left. For the middle panel, a comparison of the relative change in the amplitude of the b_H heme g_z transition is depicted in the lower left boxed portion in these antimycin-treated samples versus the H217R samples depicted in Figure 5. In each case, polar plots similar to those shown in Figures 3−6 are also shown on the right to illustrate the effects of the Q_i-site inhibitors on the orientation dependence of the EPR spectra. Spectrometer settings were as described in Figure 3.

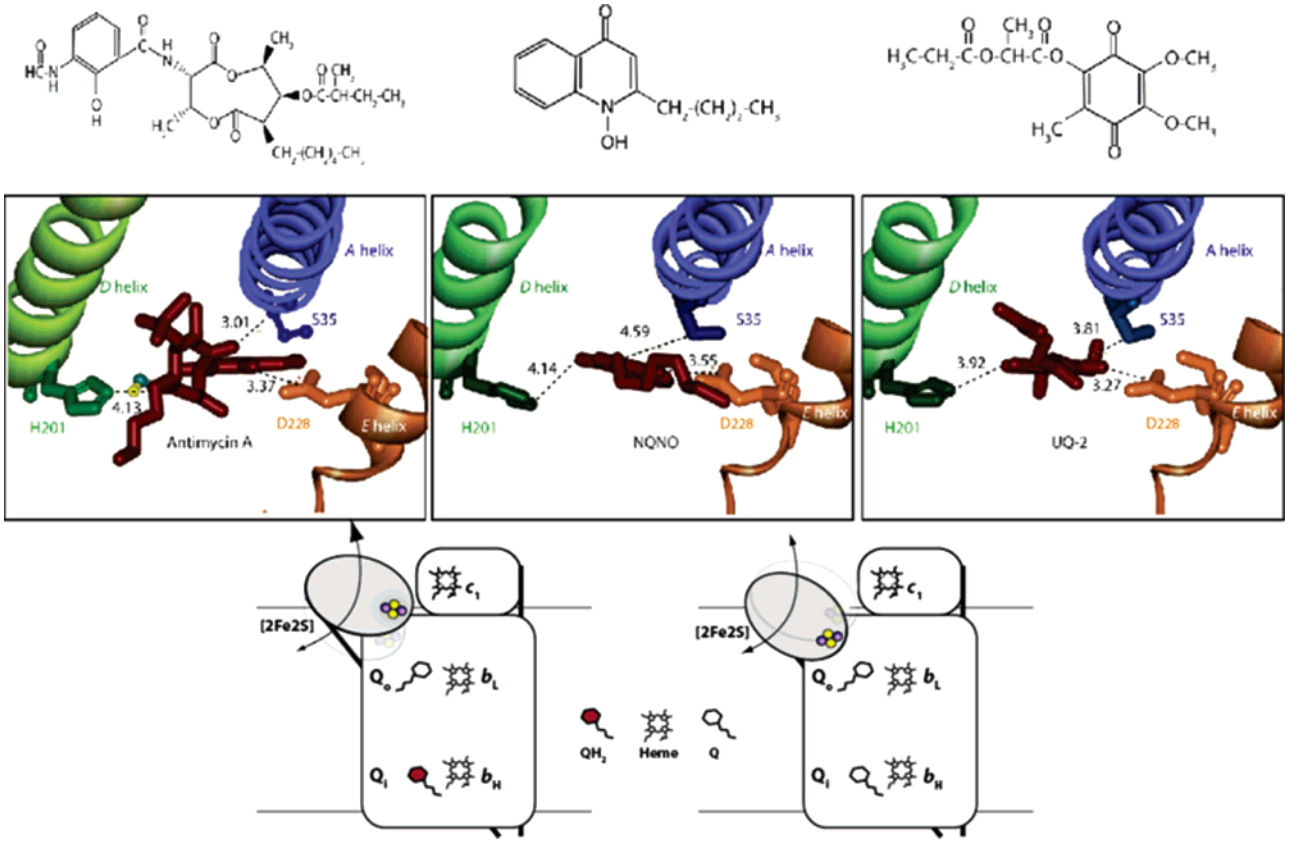

FIGURE 9: Molecular determinants for the binding of antimycin A and HQNO to the Q_i site of the cyt bc_1. The chemical structures of antimycin A, NQNO, and ubiquinone are shown in the uppermost panel. The middle panel depicts the individual interactions of these inhibitors as seen in the various crystal structures (from left to right, 1PPJ1, 1NU1, and 1NTK, respectively). Portions of the *A* (blue), *D* (green), and *E* (brown) helices surrounding the Q_i-site occupants (antimycin A, NQNO, and Q, respectively, in red) are shown. The NQNO structure shows remarkable differences with respect to its proximity to both the *A* helix Ser35 residue and the edge and propionates of the cyt b_H heme (not shown). In the lowermost panel, a cartoon is shown to depict the Q_i site occupied with either QH_2 (red ring) mimicked by antimycin A and the [2Fe−2S] cluster in a more "distal" position or Q (white ring) mimicked by HQNO and the [2Fe−2S] cluster in a more "proximal" position, to illustrate the Q_i-site occupancy structural effects on the relative mobility of the Fe/S protein at the Q_o site.

E helix has few interactions with the other helices of cyt *b* away from the N-side Q-binding niche and interacts only minimally with the carboxyl terminal TM helix of the cyt c_1 subunit. Very interestingly, it is linked directly to the solvent-exposed *ef* loop that contains the conserved PEWY sequence at the P side of the membrane (*3*, *36*, *39*), which interacts closely with the extrinsic domain of the Fe/S protein during its large-scale movement (*16*, *40*, *41*). On the other hand, NQNO, while still interacting with the *E* helix residues K251 and D252, is more distant from the I49 and H217 residues of the *A* and *D* helices, respectively, which are intimately involved in the binding of antimycin A (middle panel of Figure 9) (*33*).

Thus, binding pockets of these two inhibitors overlap but do not superimpose, as indicated by earlier works on the locations of cyt *b* mutations conferring resistance to Q_i-site inhibitors (*42*). An immediate consequence of the adjacent but structurally distinct subdomains of cyt *b* occupied by these molecules is that the structural impacts of their binding, although similar, would be nonidentical, as seen here with both native and mutant cyt bc_1. For example, antimycin A will change the conformational rigidities of the *A*, *D*, and *E* helices in a different manner than NQNO and presumably HQNO, while both of them competitively exclude Q and its derivatives from the Q_i site. Consequently, the conformational constraints inflicted by these inhibitors would be transmitted via the *A*, *D*, and *E* helices to the P side of the membrane and affect differently the conformation of the cyt *b* portion of the Q_o site and the mobility of the Fe/S protein. These expectations are in agreement with earlier studies using second-site suppressors (*38*, *41*) and steered molecular dynamics computations (*43*), which indicated that changes affecting the conformations of the *cd* and *ef* loops would affect the mobility of the Fe/S protein that interacts closely with these surface loops. Moreover, communication of the Q_i-site inhibitor occupancy through an increased rigidity of the *D* helix is in line with the alterations of the *g* transition positions observed in the EPR spectra of the cyt b_L heme upon binding of antimycin A. It has been proposed that constraining the conformation of this heme shifts its g_z value to a lower magnetic field value (*44*, *45*). Similarly, the EPR spectra of the [2Fe−2S] cluster in ordered membrane samples of the cyt b_H-less mutant H212N are consistent with a relaxation of the conformational constraints of this same *D* helix via the loss of the histidine−iron interactions of the cyt b_H heme. Consequently, even when antimycin A is added to this mutant, the changes in the position and shape of the [2Fe−2S] cluster EPR g_x transition are small, amounting to a loss in the $g_x = 1.8$ transition, and the EPR spectrum of the [2Fe−2S] cluster still retains a portion of its orientation dependence (e.g., Figure 7). Likewise, the H217L, D, and R mutations that modify the hydrogen-bonding interactions between the Q_i-site resident and the *D* helix leave behind only the strong interactions with the *E* helix. In the absence

of this interaction with antimycin A, the conformational constraint upon the *D* helix is essentially abolished, while both the changes in the line shape and orientation dependence induced by antimycin A appear enhanced. Because the interactions of HQNO and antimycin A with the H217 residue and helix *D* differ, while those with helix *E* do not, the decreased orientation dependence of the EPR spectra of the [2Fe−2S] cluster still observed in the H217 mutants upon binding of antimycin A suggests that the increased mobility of the Fe/S protein cannot solely be due to the effects transmitted via either the *D* or *E* helices (Figure 9). These considerations leave the possibility that, while the EPR spectral modifications reflecting the changing environment of the [2Fe−2S] cluster originate from different types of constraints that the Q_i-site occupants or the low-potential chain mutants apply to the *D* and *E* helices, those that decrease the orientation dependence of these spectra might be induced by interactions between antimycin A and the *A* helix of the cyt *b* at the Q_i site.

Mechanistic Implications of the Different Effects of Antimycin A and HQNO Binding on the Mobility of the Fe/S Protein at the Q_o Site. The findings that the environment and the location of the Fe/S protein change depending on the binding of different Q_i-site inhibitors or mutations severing the low potential chain of the cyt bc_1 have remarkable implications. First, it appears that, when the Q_i site is constrained via its occupancy, the equilibrium position of the reduced [2Fe−2S] cluster becomes more restricted for its interactions with Q at the Q_o site, as observed in all cases examined here. Thus, it appears that the micromobility of the Fe/S protein, possibly between the stigmatellin- and the myxothiazol-binding niches at the Q_o site, is tightly coupled to the occupancy of the Q_i site via the repositioning of the *A*, *D*, and *E* helices upon the binding of the occupants. Second, it also appears that, among the Q_i-site inhibitors and the low-potential chain mutants tested here, only antimycin A increases the mobility of the Fe/S protein maximally, as if it were to facilitate its movement away from a particular Q_o-site niche. A similar Fe/S protein mobility increase with the native enzyme is known to occur upon elimination of Q from the Q_o site either by addition of myxothiazol or by chemical Q depletion of the membranes (*28*). Therefore, it is tempting to propose that binding of antimycin A mimics a discrete state of the Q_i-site catalysis that is after the bifurcated QH_2 oxidation at the Q_o site, such as either the presence of QH_2 or absence of Q (lower panel of Figure 9). This discrete state would increase the tendency of the [2Fe−2S] cluster of the Fe/S protein to remain away from the catalytic niche of the Q_o site until the presence of an electron acceptor such as a Q or SQ inhabits the Q_i site. If this is the case, then why the second electron from the QH_2 oxidation cannot be readily taken by the reoxidized [2Fe−2S] cluster of the Fe/S protein in the presence of antimycin A could be cautiously rationalized.

In summary, oriented EPR analysis of ordered membrane samples derived from wild type and various mutants defective in the low-potential chain of the cyt bc_1, in combination with selected inhibitors, has provided evidence that binding dynamics of the Q_i-site occupants are tightly coupled to the environment and location of the [2Fe−2S] cluster of the Fe/S protein at the Q_o site. The precise molecular basis of these long distance Q_i−Q_o site interactions and their implications for the onset and maintenance of multiple turnovers of the cyt bc_1, where the mobility of the Fe/S protein is known to be crucial, now need to be addressed further.

ACKNOWLEDGMENT

We thank Drs. P. L. Dutton, C. Moser, E. A. Berry, E. Darrouzet, and D. Kramer for many helpful discussions throughout the course of this work.

REFERENCES

1. Cooley, J. W., Darrouzet, E., and Daldal, F. (2004) Bacterial hydroquinone:cyt *c* oxidoreductases: Physiology, structure, and function, in *Respiration in Archaea and Bacteria* (Zannoni, D., Ed.) Kluwer Academic Publishers, Norwell, MA.
2. Darrouzet, E., Cooley, J. W., and Daldal, F. (2004) The cytochrome bc_1 complex and its homologue the b_6f complex: Similarities and differences, *Photosynth. Res. 79*, 25−44.
3. Berry, E. A., Huang, L. S., Saechao, L. K., Pon, N. G., Valkova-Valchanova, M., and Daldal, F. (2004) X-ray structure of *Rhodobacter capsulatus* cytochrome bc_1: Comparison with its mitochondrial and chloroplast counterparts, *Photosynth. Res. 81*, 251−275.
4. Xiao, K. H., Chandrasekaran, A., Yu, L., and Yu, C. A. (2001) Evidence for the intertwined dimer of the cytochrome bc_1 complex in solution, *J. Biol. Chem. 276*, 46125−46131.
5. Berry, E. A., Guergova-Kuras, M., Huang, L. S., and Crofts, A. R. (2000) Structure and function of cytochrome *bc* complexes, *Annu. Rev. Biochem. 69*, 1005−1075.
6. Crofts, A. R., Guergova-Kuras, M., Kuras, R., Ugulava, N., Li, J. Y., and Hong, S. J. (2000) Proton-coupled electron transfer at the Q_o site: What type of mechanism can account for the high activation barrier? *Biochim. Biophys. Acta 1459*, 456−466.
7. Darrouzet, E., Moser, C. C., Dutton, P. L., and Daldal, F. (2001) Large scale domain movement in cytochrome bc_1: A new device for electron transfer in proteins, *Trends Biochem. Sci. 26*, 445−451.
8. Osyczka, A., Moser, C. C., Daldal, F., and Dutton, P. L. (2004) Reversible redox energy coupling in electron-transfer chains, *Nature 427*, 607−612.
9. Cape, J. L., Bowman, M. K., and Kramer, D. M. (2005) Reaction intermediates of quinol oxidation in a photoactivatable system that mimics electron transfer in the cytochrome bc_1 complex, *J. Am. Chem. Soc. 127*, 4208−4215.
10. Darrouzet, E., Valkova-Valchanova, M., and Daldal, F. (2000) Probing the role of the Fe−S subunit hinge region during Q_o site catalysis in *Rhodobacter capsulatus* bc_1 complex, *Biochemistry 39*, 15475−15483.
11. Xiao, K., Yu, L., and Yu, C. A. (2000) Confirmation of the involvement of protein domain movement during the catalytic cycle of the cytochrome bc_1 complex by the formation of an intersubunit disulfide bond between cytochrome *b* and the iron−sulfur protein, *J. Biol. Chem. 275*, 38597−38604.
12. Muller, F., Crofts, A. R., and Kramer, D. M. (2002) Multiple Q-cycle bypass reactions at the Q_o site of the cytochrome bc_1 complex, *Biochemistry 41*, 7866−7874.
13. de Vries, S., van Hoek, A. N., and Berden, J. A. (1988) The oxidation−reduction kinetics of cytochromes *b*, c_1, and *c* in initially fully reduced mitochondrial membranes are in agreement with the Q-cycle hypothesis, *Biochim. Biophys. Acta 935*, 208−216.
14. Wikstrom, M. K., and Berden, J. A. (1972) Oxidoreduction of cytochrome *b* in the presence of antimycin, *Biochim. Biophys. Acta 283*, 403−420.
15. van Ark, G., Raap, A. K., Berden, J. A., and Slater, E. C. (1981) Kinetics of cytochrome *b* reduction in submitochondrial particles, *Biochim. Biophys. Acta 637*, 34−42.
16. Darrouzet, E., and Daldal, F. (2002) Movement of the iron−sulfur subunit beyond the *ef* loop of cytochrome *b* is required for multiple turnovers of the bc_1 complex but not for single turnover Q_o site catalysis, *J. Biol. Chem. 277*, 3471−3476.
17. Tian, H., White, S., Yu, L., and Yu, C. A. (1999) Evidence for the head domain movement of the Rieske iron−sulfur protein in electron-transfer reaction of the cytochrome bc_1 complex, *J. Biol. Chem. 274*, 7146−7152.

18. Rieske, J. S., Baum, H., Stoner, C. D., and Lipton, S. H. (1967) On the antimycin-sensitive cleavage of complex III of the mitochondrial respiratory chain, *J. Biol. Chem. 242*, 4854−4866.
19. Gutierrez-Cirlos, E. B., and Trumpower, B. L. (2002) Inhibitory analogs of ubiquinol act anti-cooperatively on the yeast cytochrome bc_1 complex. Evidence for an alternating, half-of-the-sites mechanism of ubiquinol oxidation, *J. Biol. Chem. 277*, 1195−1202.
20. Covian, R., Gutierrez-Cirlos, E. B., and Trumpower, B. L. (2004) Anti-cooperative oxidation of ubiquinol by the yeast cytochrome bc_1 complex, *J. Biol. Chem. 279*, 15040−15009.
21. Valkova-Valchanova, M., Darrouzet, E., Moomaw, C. R., Slaughter, C. A., and Daldal, F. (2000) Proteolytic cleavage of the Fe−S subunit hinge region of *Rhodobacter capsulatus* bc_1 complex: Effects of inhibitors and mutations, *Biochemistry 39*, 15484−15492.
22. Gray, K. A., Dutton, P. L., and Daldal, F. (1994) Requirement of histidine-217 for ubiquinone reductase-activity (Q_i-site) in the cytochrome bc_1 complex, *Biochemistry 33*, 723−733.
23. Atta-Asafo-Adjei, E., and Daldal, F. (1991) Size of the amino acid side chain at position 158 of cytochrome *b* is critical for an active cytochrome bc_1 complex and for photosynthetic growth of *Rhodobacter capsulatus*, *Proc. Natl. Acad. Sci. U.S.A. 88*, 492−496.
24. Roberts, A. G., Bowman, M. K., and Kramer, D. M. (2002) Certain metal ions are inhibitors of cytochrome b_6f complex "Rieske" iron−sulfur protein domain movements, *Biochemistry 41*, 4070−4079.
25. Prince, R. C., Crowder, M. S., and Bearden, A. J. (1980) The orientation of the magnetic axes of the membrane-bound iron−sulfur clusters of spinach chloroplasts, *Biochim. Biophys. Acta 592*, 323−337.
26. Cooley, J. W., Roberts, A. G., Bowman, M. K., Kramer, D. M., and Daldal, F. (2004) The raised midpoint potential of the [2Fe−2S] cluster of cytochrome bc_1 is mediated by both the Q_o site occupants and the head domain position of the Fe−S protein subunit, *Biochemistry 43*, 2217−2227.
27. Ding, H., Robertson, D. E., Daldal, F., and Dutton, P. L. (1992) Cytochrome bc_1 complex [2Fe−2S] cluster and its interaction with ubiquinone and ubihydroquinone at the Q_o site: A double-occupancy Q_o site model, *Biochemistry 31*, 3144−3158.
28. Dervartanian, D. V., Albracht, S. P., Berden, J. A., van Gelder, B. F., and Slater, E. C. (1973) The EPR spectrum of isolated complex III, *Biochim. Biophys. Acta 292*, 496−501.
29. Darrouzet, E., Valkova-Valchanova, M., and Daldal, F. (2002) The [2Fe−2S] cluster E_m as an indicator of the iron−sulfur subunit position in the ubihydroquinone oxidation site of the cytochrome bc_1 complex. *J. Biol. Chem. 277*, 3464−3470.
30. van Ark, G., and Berden, J. A. (1977) Binding of HQNO to beef-heart sub-mitochondrial particles, *Biochim. Biophys. Acta 459*, 119−127.
31. von Jagow, G., and Link, T. A. (1986) Use of specific inhibitors on the mitochondrial bc_1 complex, *Methods Enzymol. 126*, 253−271.
32. Rich, P. R., Jeal, A. E., Madgwick, S. A., and Moody, A. J. (1990) Inhibitor effects on redox-linked protonations of the *b* haems of the mitochondrial bc_1 complex, *Biochim. Biophys. Acta 1018*, 29−40.
33. Gao, X., Wen, X., Esser, L., Quinn, B., Yu, L., Yu, C. A., and Xia, D. (2003) Structural basis for the quinone reduction in the bc_1 complex: A comparative analysis of crystal structures of mitochondrial cytochrome bc_1 with bound substrate and inhibitors at the Q_i site, *Biochemistry 42*, 9067−9080.
34. Kolling, D. R., Samoilova, R. I., Holland, J. T., Berry, E. A., Dikanov, S. A., and Crofts, A. R. (2003) Exploration of ligands to the Q_i site semiquinone in the bc_1 complex using high-resolution EPR, *J. Biol. Chem. 278*, 39747−39754.
35. Hacker, B., Barquera, B., Crofts, A. R., and Gennis, R. B. (1993) Characterization of mutations in the cytochrome *b* subunit of the bc_1 complex of *Rhodobacter sphaeroides* that affect the quinone reductase site Q_c, *Biochemistry 32*, 4403−4410.
36. Zhang, Z., Huang, L., Shulmeister, V. M., Chi, Y. I., Kim, K. K., Hung, L. W., Crofts, A. R., Berry, E. A., and Kim, S. H. (1998) Electron transfer by domain movement in cytochrome bc_1, *Nature 392*, 677−684.
37. Howell, N., and Robertson, D. E. (1993) Electrochemical and spectral analysis of the long-range interactions between the Q_o and Q_i sites and the heme prosthetic groups in ubiquinol−cytochrome *c* oxidoreductase, *Biochemistry 32*, 11162−11172.
38. Saribas, A. S., Valkova-Valchanova, M., Tokito, M. K., Zhang, Z., Berry, E. A., and Daldal, F. (1998) Interactions between the cytochrome *b*, cytochrome c_1, and Fe−S protein subunits at the ubihydroquinone oxidation site of the bc_1 complex of *Rhodobacter capsulatus*, *Biochemistry 37*, 8105−8114.
39. Palsdottir, H., Lojero, C. G., Trumpower, B. L., and Hunte, C. (2003) Structure of the yeast cytochrome bc_1 complex with a hydroxyquinone anion Q_o site inhibitor bound, *J. Biol. Chem. 278*, 31303−31311.
40. Darrouzet, E., Valkova-Valchanova, M., Moser, C. C., Dutton, P. L., and Daldal, F. (2000) Uncovering the [2Fe−2S] domain movement in cytochrome bc_1 and its implications for energy conversion, *Proc. Natl. Acad. Sci. U.S.A. 97*, 4567−4572.
41. Darrouzet, E., and Daldal, F. (2003) Protein−protein interactions between cytochrome *b* and the Fe−S protein subunits during QH_2 oxidation and large-scale domain movement in the bc_1 complex, *Biochemistry 42*, 1499−1507.
42. di Rago, J. P., and Colson, A. M. (1988) Molecular basis for resistance to antimycin and diuron, Q-cycle inhibitors acting at the Q_i site in the mitochondrial ubiquinol-cytochrome *c* reductase in *Saccharomyces cerevisiae*, *J. Biol. Chem. 263*, 12564−12570.
43. Izrailev, S., Crofts, A. R., Berry, E. A., and Schulten, K. (1999) Steered molecular dynamics simulation of the Rieske subunit motion in the cytochrome bc_1 complex, *Biophys. J. 77*, 1753−1768.
44. Salerno, J. C. (1984) Cytochrome electron spin resonance line shapes, ligand fields, and components stoichiometry in ubiquinol-cytochrome *c* oxidoreductase, *J. Biol. Chem. 259*, 2331−2336.
45. Saribas, A. S., Ding, H., Dutton, P. L., and Daldal, F. (1997) Substitutions at position 146 of cytochrome *b* affect drastically the properties of heme b_L and the Q_o site of *Rhodobacter capsulatus* cytochrome bc_1 complex, *Biochim. Biophys. Acta 1319*, 99−108.

BI050571+